Electrocatalysis Hot Paper

How to cite:
International Edition: doi.org/10.1002/anie.202003093
German Editon: doi.org/10.1002/ange.202003093

Acid–Base Interaction Enhancing Oxygen Tolerance in Electrocatalytic Carbon Dioxide Reduction

Pengsong Li, Xu Lu, Zishan Wu, Yueshen Wu, Richard Malpass-Evans, Neil B. McKeown, Xiaoming Sun,* and Hailiang Wang**

Abstract: *Hybrid electrodes with improved O_2 tolerance and capability of CO_2 conversion into liquid products in the presence of O_2 are presented. Aniline molecules are introduced into the pore structure of a polymer of intrinsic microporosity to expand its gas separation functionality beyond pure physical sieving. The chemical interaction between the acidic CO_2 molecule and the basic amino group of aniline renders enhanced CO_2 separation from O_2. Loaded with a cobalt phthalocyanine-based cathode catalyst, the hybrid electrode achieves a CO Faradaic efficiency of 71 % with 10 % O_2 in the CO_2 feed gas. The electrode can still produce CO at an O_2/CO_2 ratio as high as 9:1. Switching to a Sn-based catalyst, for the first time O_2-tolerant CO_2 electroreduction to liquid products is realized, generating formate with nearly 100 % selectivity and a current density of 56.7 mA cm^{-2} in the presence of 5 % O_2.*

Electrochemical CO_2 reduction driven by renewable energy sources is an attractive strategy for converting CO_2 into value-added carbon-based products.[1–7] If achieved on a large scale, it could help alleviate the global warming and ocean acidification issues.[8,9] For this process to be more commercially relevant, the CO_2 reactant should come from practical sources such as combustion exhaust and ambient air,[10,11] both of which contain a substantial amount of O_2. However, in a realistic electrolytic cell without mass-transport limitation, the CO_2 reduction reactions can be completely inhibited by as little as 5 % O_2 in CO_2 because of the considerable difference in their standard reduction electrode potentials.[10,12–15] It is therefore challenging yet potentially highly rewarding to develop a catalytic electrode that can directly valorize O_2-containing CO_2 gases without requiring additional energy input for reactant purification.

In our prior work, we designed the first O_2-tolerant catalytic electrode for CO_2 reduction. Our design was to integrate a CO_2 reduction electrocatalyst with a polymer of intrinsic microporosity (PIM) layer that can selectively permeate CO_2 from its O_2 mixture.[10] This electrode was able to generate CO with a Faradaic efficiency (FE) of 75.9 % from CO_2 containing 5 % O_2. Despite this progress, it is still necessary to further improve O_2 tolerance of the electrode and expand the scope of products. Considering that PIM separates CO_2 from O_2 via a physical process through its size-selective pores,[16,17] we believe there is opportunity to enhance the separation process by introducing chemical interactions.

Herein, we report a second generation of O_2-tolerant catalytic electrodes for CO_2 reduction, which are developed from their predecessors by introducing guest aniline molecules into the PIM structure and by changing the electrocatalyst. Benefiting from the chemical interaction between acidic CO_2 and the basic amino group of aniline, the PIM/aniline hybrid membrane demonstrates improved CO_2 vs. O_2 selectivity compared to pure PIM. Deployed in an electrolytic flow cell, our electrode comprising such a hybrid gas selection layer and a catalyst layer of cobalt phthalocyanine (CoPc) molecules anchored on carbon nanotubes (CNTs) achieves a FE_{CO} of 71 % in the presence of 10 % O_2 in CO_2. At a high O_2/CO_2 ratio of 9:1, the electrode can still have net CO_2 conversion, whereas the control electrode without aniline completely loses its function. Switching the catalyst to Sn particles allows us to expand our products beyond CO and realize the first selective reduction of CO_2 to formate in the presence of 5 % O_2.

We first used a gas separation experiment (see the Supporting Information for details), where a CO_2/O_2 mixture gas with a fixed volume ratio of 1:39 flows through the channel on one side of the gas diffusion electrode (GDE) and a N_2 carrier gas flows on the other side for gas sampling (Figure 1 a), to study the amounts of CO_2 and O_2 penetrating the GDE. The GDE was a carbon fiber paper (CFP) or a CFP with a gas selection layer drop-casted on the side facing the CO_2/O_2 mixture gas channel. As can be seen from the gas chromatography (GC) peak areas, the CFP alone can reject both CO_2 and O_2 to some extent (Figure 1 b,c). CFP coated with a layer of PIM can more effectively limit CO_2 and O_2 penetration and decrease the O_2/CO_2 ratio compared to the CFP-only case. When the PIM layer is infiltrated with aniline or toluene, gas (especially O_2) penetration is further suppressed. In the aniline case, we observed the smallest O_2/CO_2

[*] P. Li, Prof. Dr. X. Sun
State Key Laboratory of Chemical Resource Engineering
Beijing University of Chemical Technology
Beijing 100029 (P. R. China)
E-mail: sunxm@mail.buct.edu.cn

P. Li, Dr. X. Lu, Z. Wu, Y. Wu, Prof. Dr. H. Wang
Department of Chemistry, Yale University
New Haven, CT 06520 (USA)
and
Energy Sciences Institute, Yale University
West Haven, CT 06516 (USA)
E-mail: xu.lu@yale.edu
hailiang.wang@yale.edu

Dr. R. Malpass-Evans, Prof. Dr. N. B. McKeown
EastChem, School of Chemistry, University of Edinburgh
Edinburgh EH9 3FJ (UK)

Supporting information and the ORCID identification number(s) for the author(s) of this article can be found under: https://doi.org/10.1002/anie.202003093.

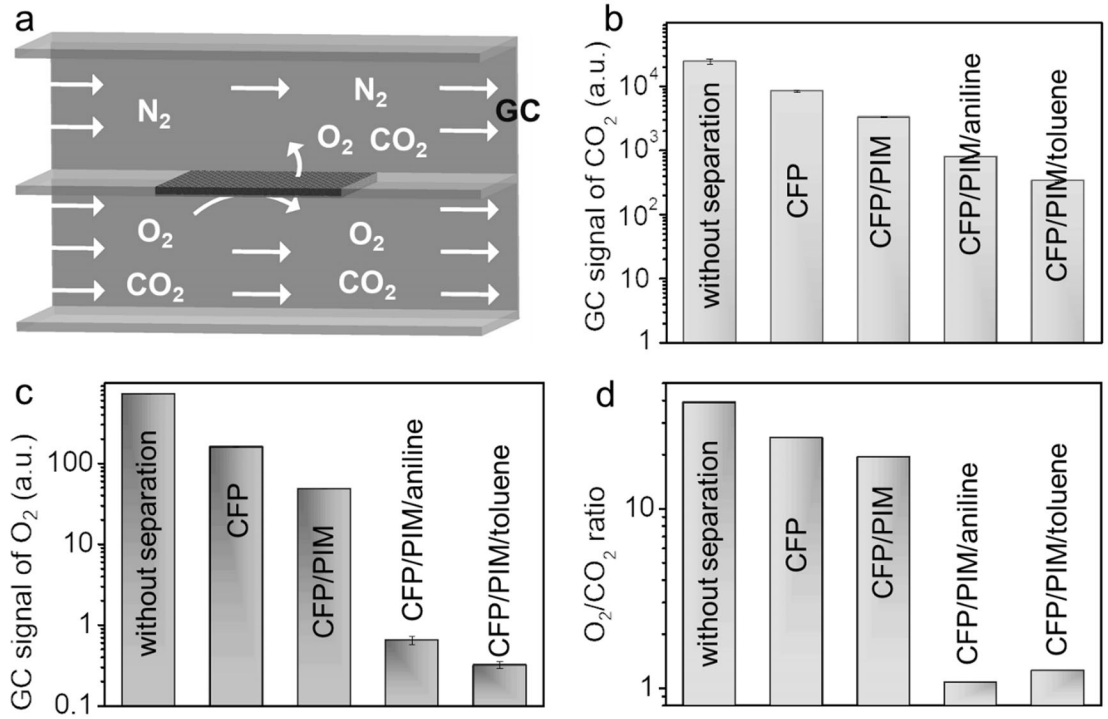

Figure 1. a) Diagram of the gas separation setup for measuring the selectivity of membrane for CO_2 separation from O_2. b) CO_2 and c) O_2 signals detected by GC for the effluent of the N_2 channel with different GDEs. Error bars represent standard deviations from multiple GC samplings. d) O_2/CO_2 volume ratios in the effluent of the N_2 channel with different GDEs.

ratio among all of the electrode configurations (Figure 1 d), revealing its highest CO_2/O_2 selectivity despite the lower CO_2 permeability caused by small molecule incorporation in the PIM structure (Figure 1 b).

We conducted infrared (IR) spectroscopy measurements to understand the enhancing effect of aniline on PIM for CO_2 separation from O_2. The IR spectra of aniline and toluene before and after 1 h of CO_2 bubbling into these two liquids are plotted in Figure 2 a–d. Interestingly, the asymmetrical stretching band of CO_2 is clearly observed at approximately 2335 cm^{-1} for the CO_2-treated aniline sample,[18,19] while no such peak is found in the case of toluene. The observation of the CO_2 peak and its decrease in wavenumber relative to a free CO_2 molecule (2349 cm^{-1})[20] indicates that CO_2 is likely adsorbed by aniline via the chemical interaction between the acidic CO_2 and the basic amino group of aniline.[21,22] In fact, amino groups are often incorporated into metal–organic framework structures to enhance their CO_2 adsorption capacity.[23,24] Figure 2 e depicts the roles played by aniline in the improved CO_2 vs. O_2 separation of the PIM/aniline material: On the one hand, the aniline molecules residing in the pore structure of PIM create a physical barrier, which enhances the rejection of the bigger O_2 (kinetic diameter 0.35 nm)[25] molecules to a greater extent compared to the smaller CO_2 (0.33 nm)[26] molecules. This would result in a lower gas permeability but a higher CO_2/O_2 selectivity. On the other hand, the amino group of aniline can selectively enhance CO_2 transport via acid–base interactions. In the absence of amino groups, the PIM/toluene membrane separates CO_2 from O_2 solely through physical sieving. Therefore, the CO_2/O_2 selectivity of PIM/toluene is higher than pure PIM but lower than PIM/aniline.

Based on the gas separation results, we anticipate the PIM/aniline-containing GDE would improve electrocatalytic CO_2 reduction in the presence of O_2, although the separation performance may not be directly translated into electrochemical performance because of their different conditions. To perform electrochemical CO_2 reduction reaction studies, we used CoPc molecules supported on CNTs (CoPc/CNT) as the catalyst,[3,10,27,28] which was coated onto the other side of the CFP supporting PIM/aniline (see the Supporting Information). A gas-diffusion electrochemical cell as reported in our previous work was used.[10,28] The cell voltage was optimized to be 3.4 V for achieving highest CO_2 reduction selectivity (Supporting Information, Figure S1). Figure 3 (Supporting Information, Figure S2) shows the FE_{CO} and total current density (j_{total}) for the reduction reactions of CO_2/O_2 mixtures containing different percentages of O_2. The PIM/aniline electrode operating with 10 % O_2 exhibits a FE_{CO} of 71 % and a j_{total} of 30.6 mA cm^{-2}, outperforming the corresponding PIM electrode which affords a FE_{CO} of 63 % under the same conditions. The improved FE_{CO} is consistent with the improved CO_2 vs. O_2 selectivity observed in the gas separation experiments (Figure 1 d). The reasonably high current density indicates that mass transport of CO_2, although suppressed by the PIM/aniline layer (Figure 1 b), is not compromising the reaction rate. In contrast, the PIM/toluene electrode, which lacks chemical interaction between toluene

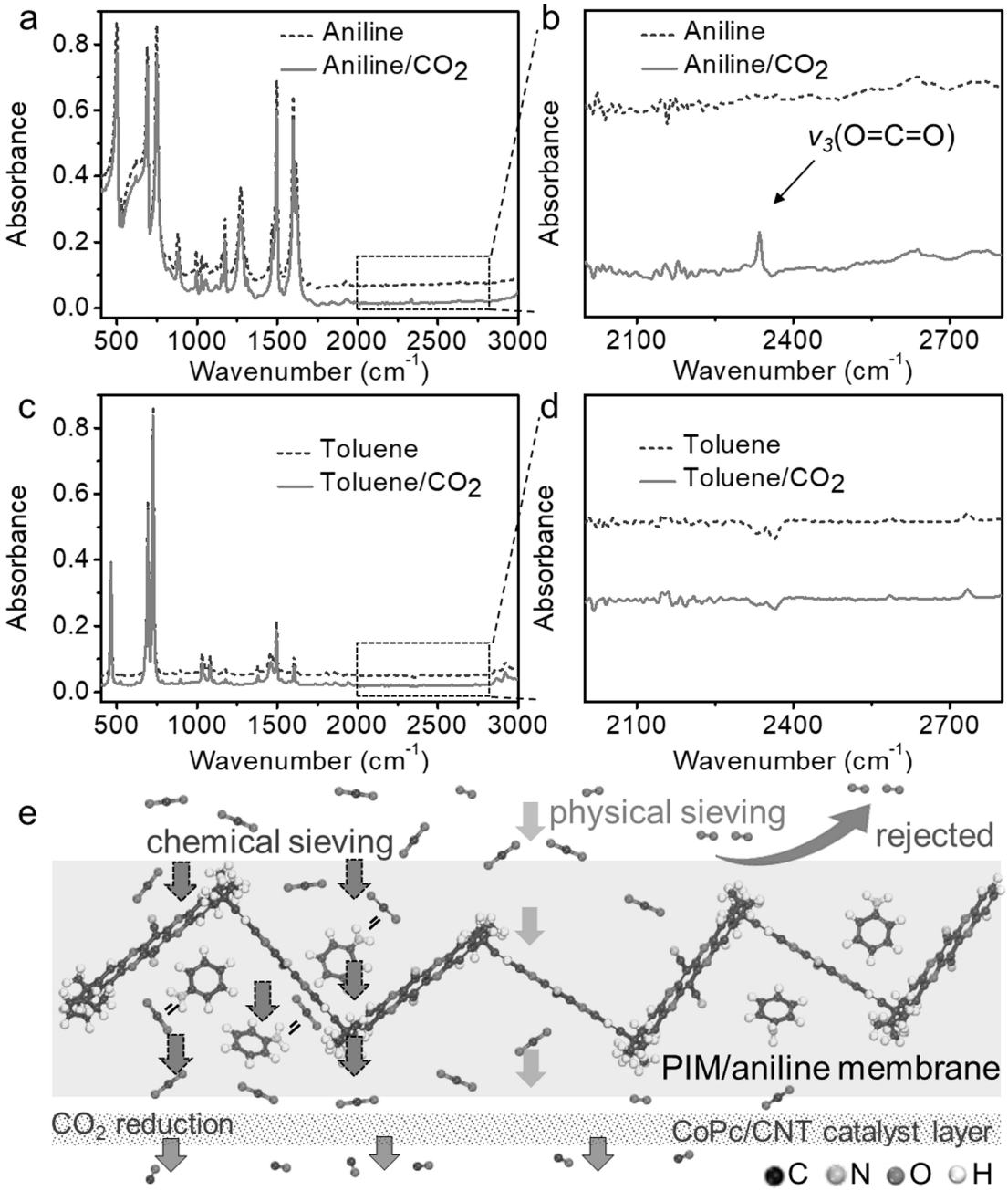

Figure 2. IR spectra of a),b) aniline and c),d) toluene before and after interacting with CO_2. e) Diagram of enhanced CO_2/O_2 separation and O_2-tolerant catalytic CO_2 reduction on a hybrid electrode with PIM/aniline.

and CO_2, shows a FE_{CO} of 33% with a j_{total} of 29.3 mA cm^{-2} at the same conditions, lower in selectivity and activity for CO production than that of the PIM electrode. The poor CO_2 reduction efficiency can be attributed to the low gas permeability of the PIM/toluene membrane, which hampers CO_2 delivery to the catalytic sites, in line with the gas separation results (Figure 1b,c). Consistently, H_2 evolution becomes more dominant (Figure 3b). For all these three catalytic electrodes, FE_{CO} gradually decreases when the O_2 content of the feed gas increases, and the PIM/aniline electrode always gives the highest FE_{CO} among the three at any fixed O_2 concentration (Figure 3a). Further control experiments with PIM/benzene (Supporting Information, Figures S3, S4) and PIM/phenol electrodes (Supporting Information, Figures S5, S6) give similar results to the PIM/toluene electrode, confirming the critical role of the amino group in the aniline molecular structure in enhancing CO_2 selection via acid–base interaction.

Incorporation of aniline in the PIM layer extends the range of O_2/CO_2 feed ratio under which the catalytic electrode can effectively convert CO_2 into CO. When operating in a gas mixture containing 40% O_2, 10% CO_2,

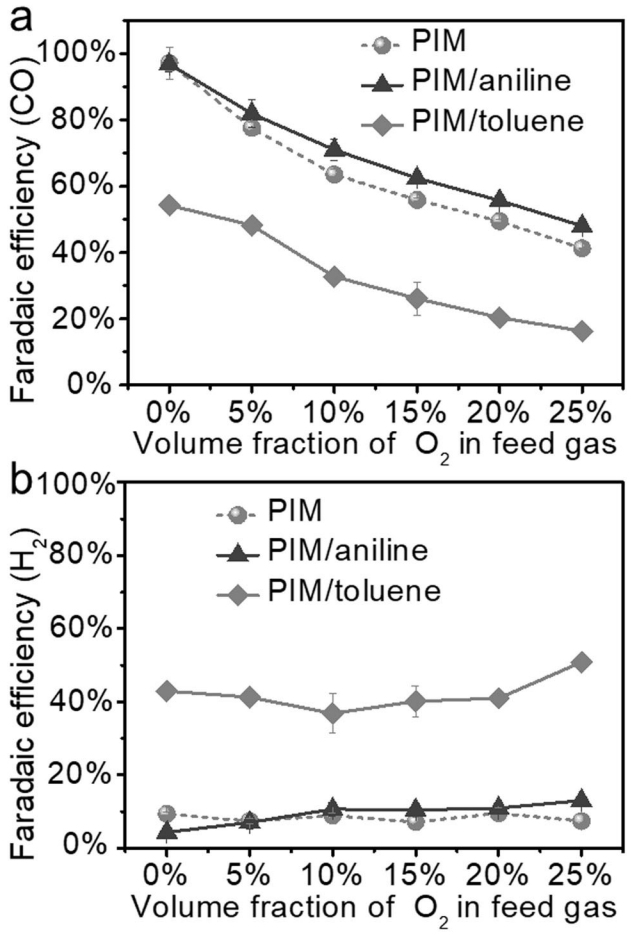

Figure 3. a) FE_{CO} and b) FE_{H_2} for PIM, PIM/aniline, and PIM/toluene cathodes operating with CO_2/O_2 feed gas containing different O_2 percentages. Electrolyte: 0.5 M aqueous $KHCO_3$; cathode catalyst: CoPc/CNT; anode catalyst: CoO_x/CNT; cell voltage: 3.4 V. Error bars represent standard deviations from multiple measurements.

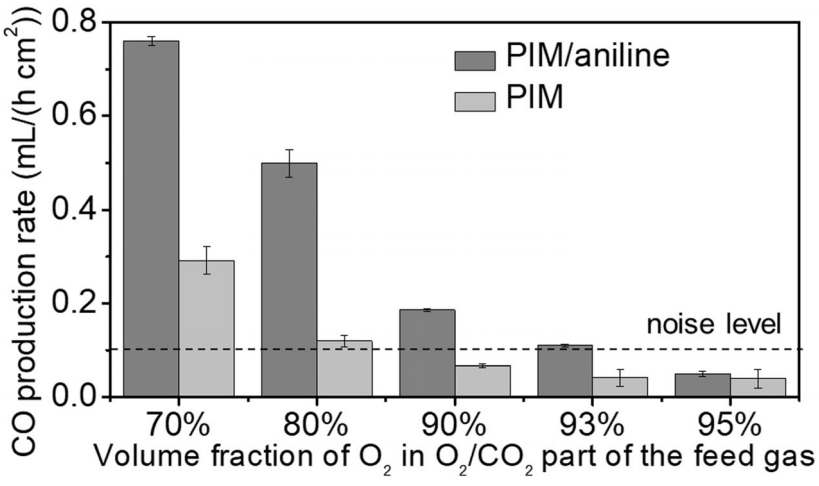

Figure 4. CO production rate vs. volume fraction of O_2 in the O_2/CO_2 part of the feed gas (CO_2, N_2, and O_2) with PIM or PIM/aniline as the CO_2/O_2 selection layer. Electrolyte: 0.5 M aqueous $KHCO_3$; cathode catalyst: CoPc/CNT; anode catalyst: CoO_x/CNT; cell voltage: 3.4 V. Volume fraction of N_2 in the feed gas is fixed at 50%. The dash line in the graph marks the noise level. Error bars represent standard deviations from multiple measurements.

and 50% N_2 (N_2 is blended in because it is a major component of air and typical flue gases[29]), the PIM electrode cannot effectively catalyze CO_2 reduction, with its measured CO production rate at the same level as the instrument noise in this case (Figure 4), whereas the PIM/aniline electrode can still produce CO at a rate that is five times higher (Figure 4). When the O_2/CO_2 ratio is further increased to 9:1, the PIM/aniline electrode can still perform CO_2 reduction at a rate significantly higher than the noise level (Figure 4). This represents another small step toward the ultimate goal of direct CO_2 valorization from the atmosphere.

The PIM/aniline gas selection layer also allows us to produce useful liquid products from electrochemical CO_2 reduction in the presence of O_2, which has never been realized before. To generate formate, we used Sn metal particles as the cathode catalyst[30] and performed electrolysis in a three-electrode cell with enhanced gas diffusion (see the Supporting Information). With 5% O_2 in the feed gas, the control Sn electrode without PIM/aniline exhibits a j_{total} up to 295.0 mA cm^{-2} (Figure 5a) but produces no formate (Figure 5b,c) at various electrode potentials. This is because O_2 reduction completely dominates the catalyst surface, in consistency with our previous observation.[10] In sharp contrast, the electrode with PIM/aniline as the gas selection layer can catalyze CO_2 reduction to formate with a FE close to 100% and a $j_{formate}$ of 56.7 mA cm^{-2} at a cathode potential of −2.4 V vs. Ag/AgCl, despite the presence of 5% O_2. As the electrode potential is further polarized to −2.8 V, $j_{formate}$ increases to 73.6 mA cm^{-2}.

In summary, we have developed a CO_2-selective layer by introducing aniline into the pores of PIM and revealed that the acid–base interaction between CO_2 and aniline enhances CO_2 separation from O_2. Loaded with CO_2 reduction electrocatalysts, the PIM/aniline catalytic electrodes show improved O_2 tolerance. CO_2 in a feed gas with an O_2/CO_2 ratio as high as 9:1 can be effectively reduced to CO. Formate can be produced at a near-unity FE and a high current density from electrochemical CO_2 reduction in the presence of O_2. The strategy of introducing chemical sieving to a gas separation membrane could be useful for directly mining the atmospheric CO_2 for fuels.

Acknowledgements

This work was supported by the National Science Foundation (Grant CHE-1651717). P.L. acknowledges an exchange student

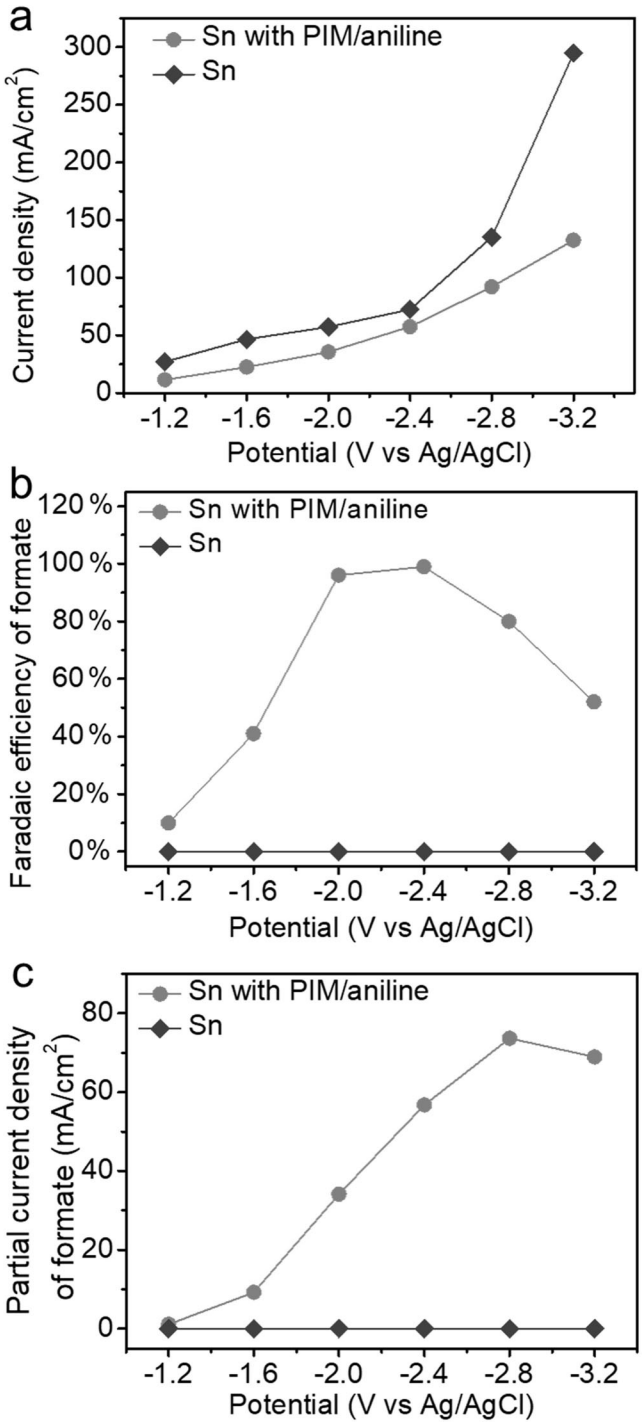

Figure 5. a) Total current density, b) formate FE, and c) formate partial current density at various cathode potentials (without *iR* correction). There is 5% O_2 in the CO_2 feed gas. Electrolyte: 0.5 M aqueous $KHCO_3$; cathode catalyst: Sn; anode catalyst: NiFe-layered double hydroxide.

fellowship from the China Scholarship Council. X.L. thanks the Croucher Fellowship for Postdoctoral Research. N.McK. acknowledges the Engineering and Physical Sciences Research Council (EPSRC EP/M01486X/1).

Conflict of interest

The authors declare no conflict of interest.

Keywords: acid–base interaction · CO_2 reduction · electrocatalysis · gas separation · O_2 tolerance

[1] Z. Weng, Y. Wu, M. Wang, J. Jiang, K. Yang, S. Huo, X. Wang, Q. Ma, G. W. Brudvig, V. S. Batista, Y. Liang, Z. Feng, H. Wang, *Nat. Commun.* **2018**, *9*, 415.
[2] P. De Luna, R. Quintero-Bermudez, C. Dinh, M. B. Ross, O. S. Bushuyev, P. Todorović, T. Regier, S. O. Kelley, P. Yang, E. H. Sargent, *Nat. Catal.* **2018**, *1*, 103 – 110.
[3] Y. Wu, Z. Jiang, X. Lu, Y. Liang, H. Wang, *Nature* **2019**, *575*, 639 – 642.
[4] J. M. Spurgeon, B. Kumar, *Energy Environ. Sci.* **2018**, *11*, 1536 – 1551.
[5] X. Lu, Y. Wu, X. Yuan, H. Wang, *Angew. Chem. Int. Ed.* **2019**, *58*, 4031 – 4035; *Angew. Chem.* **2019**, *131*, 4071 – 4075.
[6] Z. Cai, Y. Wu, Z. Wu, L. Yin, Z. Weng, Y. Zhong, W. Xu, X. Sun, H. Wang, *ACS Energy Lett.* **2018**, *3*, 2816 – 2822.
[7] D. M. Weekes, D. A. Salvatore, A. Reyes, A. Huang, C. P. Berlinguette, *Acc. Chem. Res.* **2018**, *51*, 910 – 918.
[8] S. Chu, Y. Cui, N. Liu, *Nat. Mater.* **2017**, *16*, 16 – 22.
[9] S. Nitopi, E. Bertheussen, S. B. Scott, X. Liu, A. K. Engstfeld, S. Horch, B. Seger, I. E. L. Stephens, K. Chan, C. Hahn, J. K. Nørskov, T. F. Jaramillo, I. Chorkendorff, *Chem. Rev.* **2019**, *119*, 7610 – 7672.
[10] X. Lu, Z. Jiang, X. Yuan, Y. Wu, R. Malpass-Evans, Y. Zhong, Y. Liang, N. B. McKeown, H. Wang, *Sci. Bull.* **2019**, *64*, 1890 – 1895.
[11] K. Williams, N. Corbin, J. Zeng, N. Lazouski, D. Yang, K. Manthiram, *Sustainable Energy Fuels* **2019**, *3*, 1225 – 1232.
[12] Y. Xu, J. P. Edwards, J. Zhong, C. P. O'Brien, C. M. Gabardo, C. McCallum, J. Li, C. Dinh, E. H. Sargent, D. Sinton, *Energy Environ. Sci.* **2020**, *13*, 554 – 561.
[13] P. S. Surdhar, S. P. Mezyk, D. A. Armstrong, *J. Phys. Chem.* **1989**, *93*, 3360 – 3363.
[14] A. A. Gewirth, J. A. Varnell, A. M. DiAscro, *Chem. Rev.* **2018**, *118*, 2313 – 2339.
[15] A. Bard, *Standard Potentials in Aqueous Solution*, Routledge, Abingdon-on-Thames, **2017**.
[16] P. M. Budd, K. J. Msayib, C. E. Tattershall, B. S. Ghanem, K. J. Reynolds, N. B. McKeown, D. Fritsch, *J. Membr. Sci.* **2005**, *251*, 263 – 269.
[17] M. Carta, R. Malpass-Evans, M. Croad, Y. Rogan, J. C. Jansen, P. Bernardo, F. Bazzarelli, N. B. McKeown, *Science* **2013**, *339*, 303 – 307.
[18] L. H. Jones, E. McLaren, *J. Chem. Phys.* **1958**, *28*, 995 – 995.
[19] A. L. Goodman, L. M. Campus, K. T. Schroeder, *Energy Fuels* **2005**, *19*, 471 – 476.
[20] G. Gregoire, N. R. Brinkmann, D. van Heijnsbergen, H. F. Schaefer, M. A. Duncan, *J. Phys. Chem. A* **2003**, *107*, 218 – 227.
[21] Z. Chen, S. Deng, H. Wei, B. Wang, J. Huang, G. Yu, *Front. Environ. Sci. Eng.* **2013**, *7*, 326 – 340.
[22] S. Couck, J. F. M. Denayer, G. V. Baron, T. Rémy, J. Gascon, F. Kapteijn, *J. Am. Chem. Soc.* **2009**, *131*, 6326 – 6327.
[23] B. Ghalei, K. Sakurai, Y. Kinoshita, K. Wakimoto, A. P. Isfahani, Q. Song, K. Doitomi, S. Furukawa, H. Hirao, H. Kusuda, S. Kitagawa, E. Sivaniah, *Nat. Energy* **2017**, *2*, 17086.
[24] K. Sumida, D. L. Rogow, J. A. Mason, T. M. McDonald, E. D. Bloch, Z. R. Herm, T. Bae, J. R. Long, *Chem. Rev.* **2012**, *112*, 724 – 781.

[25] P. J. M. Carrott, I. P. P. Cansado, M. M. L. R. Carrott, *Appl. Surf. Sci.* **2006**, *252*, 5948 – 5952.
[26] S. Li, J. L. Falconer, R. D. Noble, *Adv. Mater.* **2006**, *18*, 2601 – 2603.
[27] X. Zhang, Z. Wu, X. Zhang, L. Li, Y. Li, H. Xu, X. Li, X. Yu, Z. Zhang, Y. Liang, H. Wang, *Nat. Commun.* **2017**, *8*, 14675.
[28] X. Lu, Y. Wu, X. Yuan, L. Huang, Z. Wu, J. Xuan, Y. Wang, H. Wang, *ACS Energy Lett.* **2018**, *3*, 2527 – 2532.
[29] D. Aaron, C. Tsouris, *Sep. Sci. Technol.* **2005**, *40*, 321 – 348.
[30] H. Jiang, K. Moon, H. Dong, F. Hua, C. P. Wong, *Chem. Phys. Lett.* **2006**, *429*, 492 – 496.

Manuscript received: February 28, 2020
Accepted manuscript online: March 25, 2020
Version of record online: ■■ ■■, ■■■■

Communications

Electrocatalysis

P. Li, X. Lu,* Z. Wu, Y. Wu,
R. Malpass-Evans, N. B. McKeown,
X. Sun,* H. Wang* _____ ■■■■–■■■■

Acid–Base Interaction Enhancing Oxygen Tolerance in Electrocatalytic Carbon Dioxide Reduction

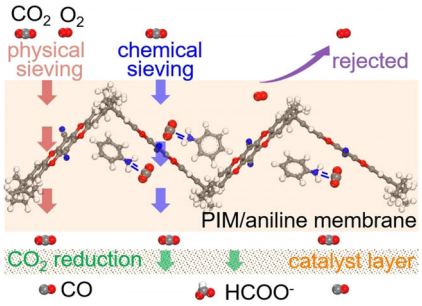

An aniline-infiltrated polymer-of-intrinsic-microporosity (PIM) membrane is reported for direct valorization of CO_2 from its mixture with O_2. The acid–base interaction between CO_2 and aniline enhances CO_2/O_2 separation, enabling catalytic electrodes capable of producing CO from a feed gas with an O_2/CO_2 ratio as high as 9:1 and of reducing CO_2 selectively to formate in the presence of O_2.